

## International Journal of Remote Sensing

Publication details, including instructions for authors and subscription information:

<http://www.tandfonline.com/loi/tres20>

### New spectral vegetation indices based on the near-infrared shoulder wavelengths for remote detection of grassland phytomass

Loris Vescovo <sup>a</sup>, Georg Wohlfahrt <sup>b</sup>, Manuela Balzarolo <sup>c</sup>, Sebastian Pilloni <sup>b</sup>, Matteo Sottocornola <sup>a</sup>, Mirco Rodeghiero <sup>a</sup> & Damiano Gianelle <sup>a</sup>

<sup>a</sup> IASMA Research and Innovation Centre, Fondazione Edmund Mach, 38010, San Michele all'Adige, Trento, Italy

<sup>b</sup> Institut für Ökologie, Universität Innsbruck, 6020, Innsbruck, Austria

<sup>c</sup> Department of Forest Environment and Resources, University of Tuscia, 01100, Viterbo, Italy

Available online: 18 Oct 2011

To cite this article: Loris Vescovo, Georg Wohlfahrt, Manuela Balzarolo, Sebastian Pilloni, Matteo Sottocornola, Mirco Rodeghiero & Damiano Gianelle (2011): New spectral vegetation indices based on the near-infrared shoulder wavelengths for remote detection of grassland phytomass, International Journal of Remote Sensing, DOI:10.1080/01431161.2011.607195

To link to this article: <http://dx.doi.org/10.1080/01431161.2011.607195>



PLEASE SCROLL DOWN FOR ARTICLE

Full terms and conditions of use: <http://www.tandfonline.com/page/terms-and-conditions>

This article may be used for research, teaching, and private study purposes. Any substantial or systematic reproduction, redistribution, reselling, loan, sub-licensing, systematic supply, or distribution in any form to anyone is expressly forbidden.

The publisher does not give any warranty express or implied or make any representation that the contents will be complete or accurate or up to date. The accuracy of any instructions, formulae, and drug doses should be independently verified with primary sources. The publisher shall not be liable for any loss, actions, claims, proceedings, demand, or costs or damages whatsoever or howsoever caused arising directly or indirectly in connection with or arising out of the use of this material.

## New spectral vegetation indices based on the near-infrared shoulder wavelengths for remote detection of grassland phytomass

LORIS VESCOVO<sup>†</sup>, GEORG WOHLFAHRT<sup>‡</sup>, MANUELA BALZAROLO<sup>§</sup>,  
SEBASTIAN PILLONI<sup>‡</sup>, MATTEO SOTTOCORNOLA<sup>†</sup>, MIRCO  
RODEGHIERO<sup>†</sup> and DAMIANO GIANELLE<sup>\*†</sup>

<sup>†</sup>IASMA Research and Innovation Centre, Fondazione Edmund Mach, 38010 San Michele  
all'Adige, Trento, Italy

<sup>‡</sup>Institut für Ökologie, Universität Innsbruck, 6020 Innsbruck, Austria

<sup>§</sup>Department of Forest Environment and Resources, University of Tuscia, 01100 Viterbo, Italy

(Received 24 June 2010; in final form 13 May 2011)

This article examines the possibility of exploiting ground reflectance in the near-infrared (NIR) for monitoring grassland phytomass on a temporal basis. Three new spectral vegetation indices (infrared slope index, ISI; normalized infrared difference index, NIDI; and normalized difference structural index, NDSI), which are based on the reflectance values in the H25 (863–881 nm) and the H18 (745–751 nm) Chris Proba (mode 5) bands, are proposed. Ground measurements of hyperspectral reflectance and phytomass were made at six grassland sites in the Italian and Austrian mountains using a hand-held spectroradiometer. At full canopy cover, strong saturation was observed for many traditional vegetation indices (normalized difference vegetation index (NDVI), modified simple ratio (MSR), enhanced vegetation index (EVI), enhanced vegetation index 2 (EVI 2), renormalized difference vegetation index (RDVI), wide dynamic range vegetation index (WDRVI)). Conversely, ISI and NDSI were linearly related to grassland phytomass with negligible inter-annual variability. The relationships between both ISI and NDSI and phytomass were however site specific. The WinSail model indicated that this was mostly due to grassland species composition and background reflectance. Further studies are needed to confirm the usefulness of these indices (e.g. using multispectral specific sensors) for monitoring vegetation structural biophysical variables in other ecosystem types and to test these relationships with aircraft and satellite sensors data. For grassland ecosystems, we conclude that ISI and NDSI hold great promise for non-destructively monitoring the temporal variability of grassland phytomass.

### 1. Introduction

#### 1.1 *The spectral vegetation indices approach and the saturation problem*

Empirical and simple remote-sensing methods are commonly used to monitor vegetation characteristics (phytomass, leaf area index (LAI), chlorophyll content, green to dead biomass ratio, etc.) (Price 1993, Gao *et al.* 2000, Van Leeuwen and Barron 2006, Gitelson *et al.* 2008). The use of spectral vegetation indices, calculated as a

---

\*Corresponding author. Email: damiano.gianelle@iasma.it

ratio or normalized difference from near-infrared (NIR, 750–1350 nm) and visible bands, has become one of the most common remote-sensing approach to retrieve biophysical variables over the past three decades (Colwell 1974, Tucker 1979, Sellers 1985, Leprieur *et al.* 1994, Boegh *et al.* 2002). Although they do not associate directly with plant biomass, spectral reflectance indices relate to the LAI, which is a proxy of phytomass (Hill 2004) and depends on canopy structure, density and non-photosynthetic vegetation components. However, accurate estimates of biophysical variables at full canopy cover are still problematic, as most spectral vegetation indices tend to saturate under these conditions (Tucker 1977, Myneni *et al.* 1995, Gitelson *et al.* 1996).

To solve the saturation problem, many indices that use the red and the NIR bands have been implemented through a linearization of the relationship with quantitative biophysical variables (e.g. the wide dynamic range vegetation index (WDRVI) (Gitelson 2004); the renormalized difference vegetation index (RDVI) (Roujean and Breon 1995); and the modified simple ratio (MSR) (Chen 1996)). To enhance the vegetation signal with improved sensitivity in full canopy regions, the enhanced vegetation index (EVI; Liu and Huete 1995) was designed using the red and NIR bands as the previous indices but with the addition of the blue band. The EVI improved vegetation monitoring through a de-coupling of the canopy background signal and a reduction in atmospheric influences. For these reasons, the EVI was adopted as a standard Moderate Resolution Imaging Spectroradiometer (MODIS) product and it has become very popular with users. In addition, a modified two-band EVI index (EVI 2) has recently been proposed with the aim of providing an index whose performance is comparable to EVI, when the blue band is not available or the signal quality in the blue band is low (Jiang *et al.* 2008). However, it is still unknown whether EVI, EVI 2 or any other single index has completely achieved the aforementioned objectives, which is crucial as the uncertainties involved in parameter estimation at full canopy cover can result in significant errors at regional and global scales. For example, in carbon credit budgeting, there is a need for improving the estimation accuracy of vegetation biophysical characteristics to avoid erroneous estimates of carbon terrestrial sinks (Prince 1991, Rosenqvist *et al.* 2003).

The use of the short-wave infrared (SWIR, 1350–2500 nm) region of the spectrum for predicting biophysical vegetation variables is another promising approach to overcome the saturation problem in predicting biophysical vegetation variables. The SWIR bands relate well to canopy water content (Everitt *et al.* 1989, Ustin *et al.* 2004) and since the canopy liquid water absorption of radiation linearly relates to the LAI, it can be seen as a proxy for estimating vegetation biomass from remote-sensing platforms. Despite being proposed many years ago, vegetation indices based on SWIR bands have not been used much because of the generally high cost of sensors that provide SWIR data (Ustin *et al.* 2004).

## 1.2 The role of the near-infrared wavelengths in canopy remote sensing

NIR reflectance spectroscopy has proved to be very effective for the analysis of grassland biophysical parameters (e.g. above-ground biomass, proportion of dead material), or other plant traits (e.g. nitrogen content and leaf mass ratio; Pilon *et al.* 2010). The red-edge spectral region (680–740 nm), the peak of maximum reflectance region (900 nm) and the moisture-sensitive feature around 970 nm have been widely investigated in the literature. However, little attention has been given to the slope in the 750–900 nm waveband, which has been considered a region of near-uniform

reflectance throughout the so-called NIR shoulder. Reflectance in the NIR region is related to many leaf structural features such as intercellular air spaces, the ratio of the mesophyll per unit leaf area, the ratio between palisade mesophyll and spongy mesophyll, leaf pubescence, leaf cuticles and dry matter content (Knipling 1970, Delucia and Nelson 1993, Slaton *et al.* 2001, Jacquemoud *et al.* 2009). At canopy level, reflectance in the NIR region was found to be related to the LAI, the leaf angle distribution (LAD) and the background reflectance (Jacquemoud *et al.* 2009). A change in the slope of spectral signatures from 780 to 940 nm was observed during different development stages in crop canopies by Thenkabail *et al.* (2000). As suggested by Pinty *et al.* (2009), when dealing with full canopy cover it is very important to focus on the NIR wavelengths, because changes in the reflectance in the NIR domain can still be observed, due to the multiple scattering processes typical of large canopy optical depths.

In the past few years, there has been increasing attention on ground spectrometric observations, which avoid problems associated with airborne and satellite measurements, such as the need for atmospheric corrections, mismatch in spatial scale as compared to ecosystem measurements (e.g. eddy covariance), changes in viewing geometry and limited temporal resolution. These so-called scale-appropriate spectral measurements (Gamon *et al.* 2006) are a fundamental step in up-scaling observations from the ecosystem to larger scales.

### 1.3 Hypotheses and objectives of this study

The objective of the present study is to test the suitability of vegetation indices, based on reflectance in the NIR region, for remote monitoring of the temporal variability of grassland phytomass. More specifically the aims are to:

1. investigate the relationships between the infrared slope index (ISI), the normalized infrared difference index (NIDI), the normalized difference structural index (NDSI) and phytomass at different grassland sites, and to compare these to 'traditional' indices with regard to saturation at full canopy cover;
2. test the influence of canopy variables (species composition, leaf orientation, canopy background) on the relationships between phytomass versus ISI, NIDI and NDSI using a modelling approach.

According to the observations of Thenkabail *et al.* (2000), and to the signature temporal trends observed in our previous work (Gianelle *et al.* 2009), we hypothesize that the proposed indices, which exploit reflectance in the NIR shoulder region, saturate much less at full canopy cover and will exhibit a superior performance as compared to traditional indices.

## 2. Methods

### 2.1 Study sites

The main study site, Monte Bondone (table 1), is located at 1550 m a.s.l. on a mountain plateau in the Italian Alps (Viote del Monte Bondone). The area is managed as an extensive meadow and is dominated by *Nardus stricta* (characterized by hard, thin, needle-like leaves). The climate of this area is sub-continental (warm and wet summer), with precipitation peaks in spring and autumn. Measurements at the Monte Bondone site were collected in 2005 and 2006 on a 1 m spectral footprint corresponding to previous high spatial resolution biomass maps (1 m) obtained by

Table 1. Characteristics of the investigated grasslands.

	Monte Bondone	Amplero	Neustift	Längenfeld	Leutasch	Scharnitz
Latitude	46° 01'	41° 00'	47° 07'	47° 03'	47° 22'	47° 23'
Longitude	11° 04'	13° 22'	11° 19'	10° 57'	11° 09'	11° 15'
Elevation (m)	1550	900	970	1180	1115	964
Mean annual temperature (°C)	5.5	10.0	6.5	5.8	4.8	6.4
Mean annual precipitation (mm)	1189	1365	852	733	1309	1418
Snow cover (days)	134–154 (2005–2006)	60–100 (2005–2006)	93–128 (2005–2006)	85–138 (2005–2006)	87–148 (2005–2006)	73 (2006)
Vegetation type	<i>Nardetum alpinum</i> Typic Hapludalfs Hay meadow	<i>Seslerietum apenninae</i> Haplic Phaeozem Hay meadow/pasture	<i>Pastinaco-Arrhenatheretum</i> Gleyic Fluvisol Hay meadow	<i>Phyteumo-Trisetion</i> Gleyic Fluvisol Hay meadow	<i>Astrantio-Trisetum</i> Rendzic Leptosol Hay meadow	<i>Arrhenatherum montanum</i> Rendzic Leptosol Hay meadow
Soil type						
Management						
Cuts/year	1	1	3	3	2	2
Fertilization	None	None	Solid/liquid manure	Solid/liquid manure	Solid/liquid manure	Solid/liquid manure
Main plant species	<i>Nardus stricta</i> , <i>Avenella flexuosa</i> , <i>Koeleria pyramidata</i> , <i>Poa violacea</i> , <i>Festuca rubra</i>	<i>Sesleria apennina</i> , <i>Echtranthus graminifolius</i> , <i>Pedicularis elegans</i> , <i>Festuca ovina</i>	<i>Dactylis glomerata</i> , <i>Festuca pratensis</i> , <i>Phleum pratensis</i> , <i>Trisetum flavescens</i> , <i>Trifolium</i> sp.	<i>Alopecurus pratensis</i> , <i>Trisetum flavescens</i> , <i>Achillea millefolium</i> , <i>Alchemilla vulgaris</i> , <i>Rumex acetosa</i>	<i>Dactylis glomerata</i> , <i>Trisetum flavescens</i> , <i>Alchemilla vulgaris</i> , <i>Geranium sylvaticum</i>	<i>Arrhenatherum elatius</i> , <i>Festuca pratensis</i> , <i>Tragopogon pratensis</i>

an Advanced Spectroscopic Imaging System (ASPIS) airborne sensor (Vescovo and Gianelle 2006). During 2006, spectral and biophysical measurements were carried out in five other grassland sites (table 1), one in Italy (Amplero) and four in Austria (Neustift, Scharnitz, Leutasch and Längenfeld). All study sites were, or still are, subject to research activities in both national and European projects (e.g. Carbomont, CarboEurope-IP and GHG-Europe).

The Austrian grassland sites are located in the Tyrolean Alps (western Austria) and are intensively managed as hay meadows. Their composition includes species typical of intensively managed grasslands, such as *Dactylis glomerata*, *Festuca pratensis*, *Arrhenatherum elatius*, *Trifolium* sp., *Taraxacum officinalis* and *Ranunculus acris* (mainly characterized by wider leaves). The climate of this area is continental/Alpine, with precipitation peaks during the summer (July). The Amplero site is located on the Appennines, in the Abruzzo region (central Italy) and is extensively managed as a Mediterranean mountain grassland. The climate is characterized by mild, rainy winters and dry summers, with a high grassland curing rate (the percentage of dead grass). The grassland composition includes *Festuca ovina* and *Sesleria apennina* (characterized by very thin and hard leaves). At each site, the footprint selected for measurements was homogeneous and representative of the grassland phytosociological composition and phytomass.

## 2.2 Spectral and biophysical measurements

Canopy reflectance and zenith sky irradiance were measured using a FieldSpec HandHeld ASD spectroradiometer (ASD, Inc., Boulder, CO, USA) placed on a tripod at a height of 1.5 m. This height was chosen to keep the operator out of the instrument's field of view. The tripod had a rotating horizontal arm to ensure that the spectroradiometer took measurements alternately from the vegetation and from the sky. The spectroradiometer wavelength range was between 325 and 1075 nm (spectral resolution 3 at 700 nm). Each spectrum was automatically calculated and stored by the spectroradiometer as an average of 20 readings. Canopy reflectance,  $R$ , was calculated as the ratio between the nadir vegetation radiance ( $L_{\text{veg}}$ ) and the zenith sky irradiance ( $E$ ):

$$R = \frac{L_{\text{veg}}}{E}. \quad (1)$$

For each sampling date, canopy reflectance was estimated with a cosine diffuser foreoptic (Gianelle *et al.* 2009) to consider a larger footprint of the nadir/zenith measurements. On each sampling date, five spectra of the same area were recorded. The Monte Bondone and Amplero grassland sites are cut once per year and measurements were taken from the early growing stage up to the cutting date. For the Austrian sites, which are cut 2 or 3 times during the season, the spectral measurements were taken 1–2 times per week both before and after the cut dates.

Grassland above-ground phytomass was sampled during the 2005 (14 dates) and 2006 (12 dates) growing seasons at Monte Bondone and during the 2006 growing season at all the other sites (at least on 7 dates). At all sites, above-ground phytomass samples (five replicates of 0.3 m × 0.3 m) were collected within the spectroradiometer footprint area, oven-dried and weighted.

Although a reduced sensitivity of the phytomass estimates from the spectral data was expected, due to the presence of dead plant matter, we considered phytomass to be a good approximation of green biomass (Thenkabail *et al.* 2000) given the

generally very high ratios of live material observed at most of the investigated sites. From the recorded spectral signatures, the spectral vegetation indices which are used for their linear relationship with structural biophysical variables without saturation problems were calculated simulating the Chris Proba bands (mode 5; <http://earth.esa.int/object/index.cfm?fobjectid=1488>) and then compared with the indices proposed in this article (table 2). The ISI was calculated as the difference between the reflectance values,  $\rho$ , in the H25 (863–881 nm) and the H18 (745–751 nm) Chris Proba bands. The NIDI was calculated as a normalized difference between the reflectance values in the same bands. The NDSI was calculated by multiplying NIDI with NDVI.

NDVI, MSR, EVI, RDVI, WDRVI and EVI2 were calculated from Chris Proba (mode 5) simulated bands (H25 ( $\rho_{\text{NIR}}$ ) = 863–881 nm; H7 ( $\rho_{\text{red}}$ ) = 656–666 nm; and H2 ( $\rho_{\text{blue}}$ ) = 486–495 nm) as detailed in table 2.

### 2.3 Modelling

The WinSAIL (scattering by arbitrarily inclined leaves) model (version 1.00.04 for Windows, developed by Hunt and Roberts, USDA Agricultural Research Service, Hydrology and Remote Sensing Laboratory, Beltsville, MD, USA) was utilized to analyse the role of canopy characteristics (i.e. species composition, leaf orientation and background reflectance) on the investigated relationships between ISI, NIDI, NDSI and phytomass. The model was run using different species spectral signatures (of *N. stricta*, *Festuca rubra* and *D. glomerata*), which were measured in the laboratory with a HandHeld ASD spectroradiometer and an integrating sphere. *N. stricta* has thin needle-like hard leaves, while *F. rubra* and *D. glomerata* are characterized by wider leaves. Effects of different LAD functions were also considered by simulating planophile, erectophile and plagiophile LADs. Finally, different soil reflectances (siliceous gravel and limestone sand) were measured in the field with the ASD spectroradiometer and used as an input to the WinSail model. The model was run for LAI values from 0.75 to 7 (0.75, 1, 1.5, 2, 2.5, 3, 4, 5, 6, 7) in three sets of simulations, which varied the leaf optical properties, LAD and background reflectance while keeping all other parameters constant.

## 3. Results and discussion

### 3.1 Performance of traditional vegetation indices

In the first part of this article, the performance of a number of visible–NIR indices frequently used in the literature for monitoring phytomass variation were compared. At Monte Bondone, the phytomass values increased from 90 to 204 g m<sup>-2</sup> and from 53 to 214 g m<sup>-2</sup> during the 2005 and 2006 growing seasons, respectively. For all the investigated indices, saturation occurred earlier than had been previously reported (figure 1; Tucker 1977, Myneni *et al.* 1995, Gitelson *et al.* 1996, Ustin *et al.* 2004, Vescovo and Gianelle 2006). Significant linear regressions were found only in 2006, with coefficient of determination ( $R^2$ ) values between 0.36 (MSR) and 0.57 (EVI 2). Coefficients of determination for logarithmic regressions were always higher than linear ones, indicating an obvious saturation effect (table 3). Spectral vegetation indices such as NDVI, MSR and EVI became saturated when phytomass values reached 100 g m<sup>-2</sup> (corresponding to LAI of about 1). Other indices such as EVI 2, RDVI and WDRVI showed a similar performance (figure 1).

Table 2. Summary of the vegetation indices' characteristics.

Index acronym	Algorithm	Description and use	Reference
NDVI: Normalized difference vegetation index	$\text{NDVI} = \frac{(\rho_{\text{NIR}} - \rho_{\text{red}})}{(\rho_{\text{NIR}} + \rho_{\text{red}})}$	One of the most used indexes for biomass estimation. The values are normalized for the amount of incident radiation, reducing the impact of factors such as slope and aspect.	Rouse <i>et al.</i> (1974)
MSR: Modified simple ratio	$\text{MSR} = (\rho_{\text{NIR}} / \rho_{\text{red}} - 1) / ((\rho_{\text{NIR}} / \rho_{\text{red}})^{1/2} + 1)$	It aims to linearize the relationships between the index and biophysical parameters.	Chen (1996)
EVI: Enhanced vegetation index	$\text{EVI} = 2.5 \frac{(\rho_{\text{NIR}} - \rho_{\text{red}})}{7.5\rho_{\text{blue}} + 1} / (\rho_{\text{NIR}} + 6\rho_{\text{red}} - \text{reduction in atmosphere influences.})$	Improved sensitivity in high biomass regions, de-coupling of canopy background signal and reduction in atmosphere influences.	Liu and Huete (1995)
RDVI: Renormalized difference vegetation index	$\text{RDVI} = (\rho_{\text{NIR}} - \rho_{\text{red}}) / (\rho_{\text{NIR}} + \rho_{\text{red}})^{1/2}$	It aims to linearize the relationships between the index and biophysical parameters.	Roujean and Breon (1995)
WDRVI: Wide dynamic range vegetation index	$\text{WDRVI} = (a' \rho_{\text{NIR}} - \rho_{\text{red}}) / (a' \rho_{\text{NIR}} + \rho_{\text{red}})$	It aims to linearize the relationships between the index and biophysical parameters. <i>a</i> is a weighting coefficient (<1) to decrease the disparity between the contributions of $\rho_{\text{NIR}}$ and the $\rho_{\text{red}}$ to the NDVI.	Gitelson (2004)
EVI 2: Enhanced vegetation index (two bands)	$\text{EVI 2} = 2.5 \frac{(\rho_{\text{NIR}} - \rho_{\text{red}})}{(\rho_{\text{NIR}} + 2.4\rho_{\text{red}} + 1)}$	It aims to linearize the relationships between the index and biophysical parameters, utilizing only the NIR and red bands when the blue band is not available (EVI).	Jiang <i>et al.</i> (2008)

(Continued)

Table 2. (*Continued*)

Index acronym	Algorithm	Description and use	Reference
ISI: Infrared slope index	$ISI = \rho'_{\text{NIR}} - \rho_{\text{H18}}$	It aims to linearize the relationship between the index and structural parameters (Phytomass, LAI).	This article
NIDI: Normalized infrared difference index	$NIDI = (\rho'_{\text{NIR}} - \rho_{\text{H18}}) / (\rho'_{\text{NIR}} + \rho_{\text{H18}})$	It aims to linearize the relationship between the index and structural parameters and to avoid the site specificity of the index.	This article
NDSI: Normalized difference structural index	$NDSI = (NIDI) \times (NDVI)$	It aims to linearize the relationship between the index and structural parameters integrating information from the NIR shoulder and the red bands.	This article

Notes: NDVI, MSR, EVI, RDVI, WDRVI and EVI 2 were calculated from Chris Proba (mode 5) simulated bands: H25 ( $\rho_{\text{NIR}}$ ) = 863–881 nm; H7 ( $\rho_{\text{red}}$ ) = 656–666 nm; and H2 ( $\rho_{\text{blue}}$ ) = 486–495 nm. ISI and NIDI were calculated from simulated bands H18 (745–752 nm) and H25 ( $\rho_{\text{NIR}}$ ) = 863–881 nm.

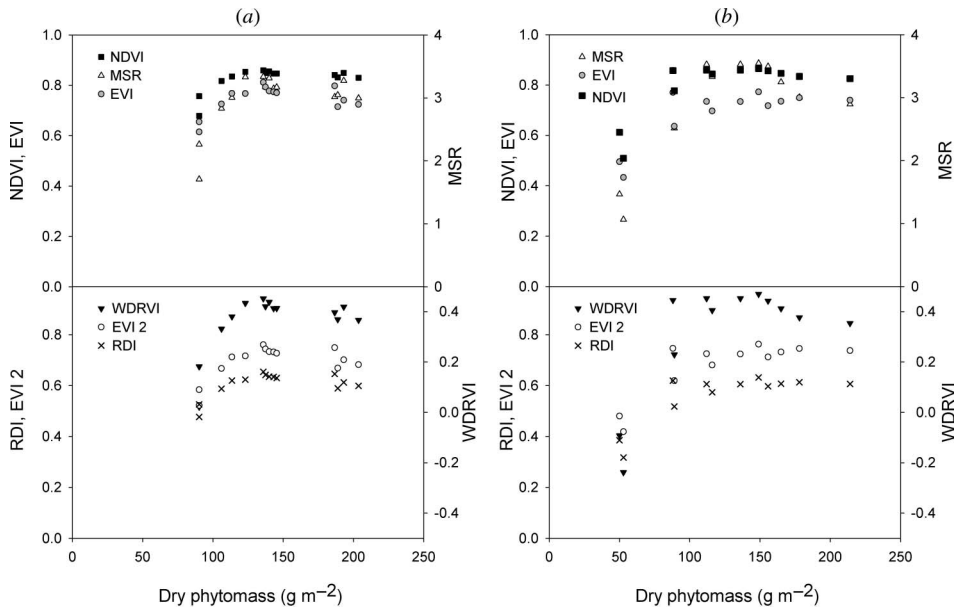


Figure 1. Spectral vegetation indices as a function of phytomass at the Monte Bondone site during (a) 2005 and (b) 2006.

Table 3. Correlation coefficients and *p*-values of linear and logarithmic index – phytomass regressions.

	2005				2006			
	Linear		Logarithmic		Linear		Logarithmic	
	<i>R</i> <sup>2</sup>	<i>p</i>						
NDVI	0.28	0.051	<b>0.38</b>	0.018	<b>0.44</b>	0.025	<b>0.63</b>	0.003
EVI	0.13	0.200	0.21	0.092	<b>0.52</b>	0.012	<b>0.69</b>	0.001
WDRVI	0.27	0.052	<b>0.38</b>	0.018	<b>0.43</b>	0.026	<b>0.63</b>	0.003
MSR	0.28	0.051	<b>0.38</b>	0.017	<b>0.36</b>	0.049	<b>0.56</b>	0.007
RDI	0.21	0.093	<b>0.31</b>	0.036	<b>0.53</b>	0.010	<b>0.71</b>	0.001
EVI2	0.20	0.099	<b>0.30</b>	0.039	<b>0.57</b>	0.007	<b>0.73</b>	0.0007

Note: Bold values represent significant regressions with *p* < 0.05.

### 3.2 Reflectance trends in the visible and NIR

The saturation effect of the indices can be examined by looking at the trend of the spectral signatures, which appeared to partition into two different phases, corresponding to the first and to the second part of the growing season (figure 2(a), where three key signature dates are shown). During the first part of the season (from A – early May to B – mid-June), as expected, the spectral signatures showed a general decrease in reflectance in the visible and an increase in the NIR regions. This first phase is consistent with a decrease of the red and increase of the NIR reflectance related to early canopy development, before full cover is achieved (Myneni *et al.* 1995). It is well-known throughout the literature that the decrease in reflectance in the visible region is

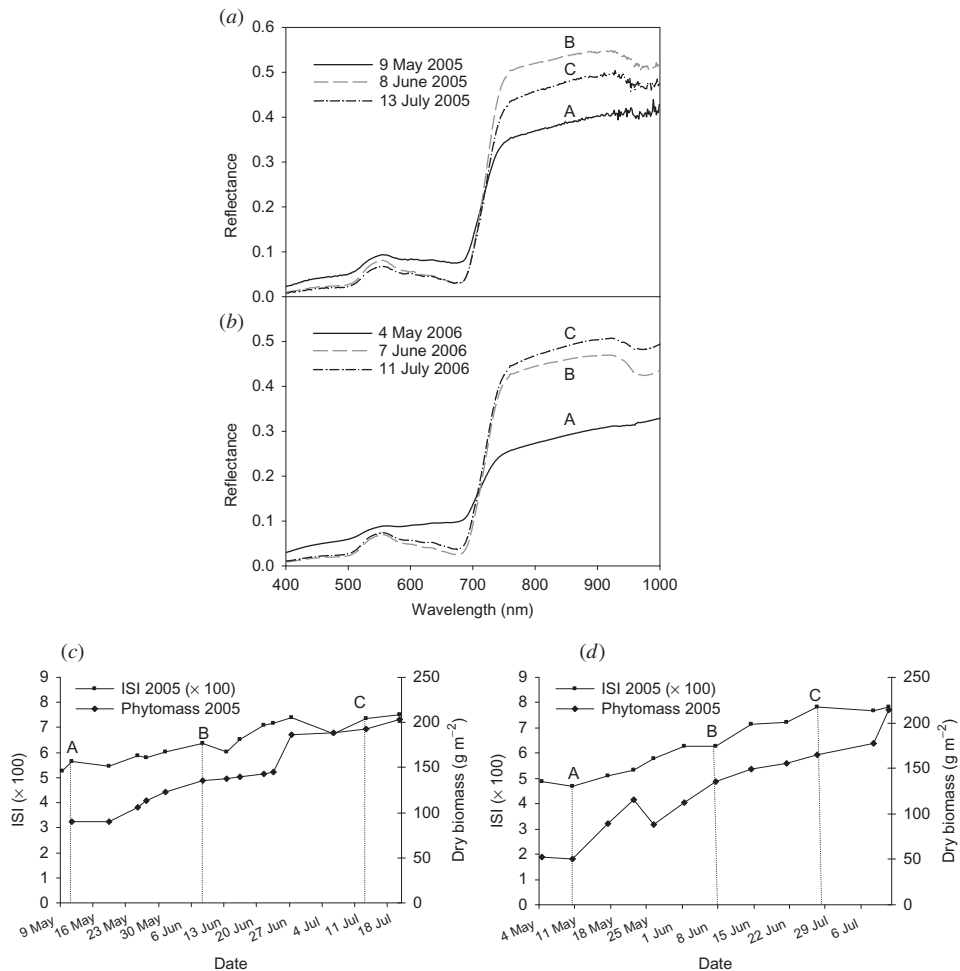


Figure 2. Grassland spectral signatures and temporal variation of ISI and phytomass during 2005 ((a) and (c), respectively) and 2006 ((b) and (d), respectively) at the Monte Bondone site. A indicates early May, B mid-June and C mid-July.

due to an increase in absorbance by the rapidly growing canopy and the presence of pigments in the leaf tissues such as chlorophyll-*a*, chlorophyll-*b* and carotenoids (e.g. Sellers 1985). The refractive-reflective scattering in the NIR is principally due to the air in the leaf cell walls and to the differences in the leaf cellular constituents' refractive indices. NIR reflectance increases during canopy development due to the higher density of plant tissues in the canopy. As shown by Liu *et al.* (2004), the increase in NIR spectral reflectance is due to the effect of plant water content on the leaf internal structure. During the second part of the season, while the phytomass and LAI were still increasing (figure 2(a), from B – mid-June to C – early July), signatures did not show noteworthy differences in the visible wavelengths, indicating saturation of the signal. On the other hand, the 750–900 nm reflectance values decreased in 2005 and were quite stable in 2006, while a considerable change in the NIR shoulder slope could be observed both in 2005 and 2006. The slope change was more evident in 2006

(figure 2(b)), when differences between the 7 June and 11 July signature were negligible in the 750 nm region, but comparably high (0.136) at 900 nm, due to an increase in the slope, which is clearly following the phytomass and LAI trends (figure 2(c) and (d)).

### 3.3 The performance of the proposed indices

The performance of the proposed indices (ISI, NIDI and NDSI) together with NDVI are shown in figure 3, where their 2005 and 2006 combined values are plotted against phytomass, for the Monte Bondone site. ISI correlated linearly to phytomass ( $R^2 = 0.86$ ;  $p < 0.001$ ). Conversely, the NIDI index (which is calculated as a normalized difference) values were quite high (up to 0.080) at the beginning of the vegetative period, when phytomass was around  $50 \text{ g m}^{-2}$ . This is likely to be due to the strong soil background scattering effect at lower canopy cover, which seems to affect the normalized index. The NIDI index reached a minimum at phytomass values around  $100 \text{ g m}^{-2}$ , followed by a linear increase at higher phytomass rates. At the same time, the minimum NDVI was 0.51 at low canopy cover, and reached a plateau of 0.82–0.86 for phytomass values higher than  $100 \text{ g m}^{-2}$ . While NDVI maintained a linear relationship for lower phytomass rates and saturated at full canopy cover, NIDI showed a linear trend only at full canopy cover. Due to the complementarity of the observed NDVI and NIDI trends, NDSI (which is calculated as NIDI multiplied by NDVI) showed a linear trend, with a  $R^2 = 0.79$ . According to these results, ISI and NDSI appear to be promising indices for phytomass estimation. ISI, which is a simple difference index, showed a higher linear correlation coefficient. NDSI also showed a significant correlation with phytomass, coupling the sensitivity of NDVI to vegetation greenness at low canopy cover with the linear response of the normalized difference index NIDI at full canopy cover.

Since the 2005 and 2006 ISI and NDSI versus dry phytomass regressions do not have significantly different slopes and intercepts (data not shown), the ISI and NDSI relationships for the observed grasslands are probably not year dependent, although more measurements are needed to confirm this hypothesis. To analyse the site dependency of ISI and NDSI in monitoring grassland phytomass, data from the Amplero, Neustift, Längenfeld, Leutasch and Scharnitz sites were also considered (figure 4). These sites were much more productive than the Monte Bondone site (figure 4(a)) since they were intensively fertilized and located at lower altitudes; in fact, phytomass in three of these sites exceeded  $600 \text{ g m}^{-2}$ .

The relationships between ISI and dry phytomass were linear and showed significant correlations at all sites ( $R^2$  ( $p$ -values): Amplero 0.65 ( $<0.01$ ), Neustift 0.78 ( $<0.001$ ), Längenfeld 0.79 ( $<0.001$ ), Leutasch 0.78 ( $<0.001$ ) and Scharnitz 0.78 ( $<0.001$ )). According to the analysed data, phytomass up to  $700 \text{ g m}^{-2}$  can be estimated without saturation effects. On the other hand, as can be inferred from the differing slopes and  $y$ -intercepts of the linear fits, the ISI–phytomass relationships appear to be site specific. NIDI did not show any significant correlation with biomass at the different sites: normalization of the ISI difference index did not overcome the site-specificity issue as expected. The NDSI was significantly correlated with phytomass at the different sites, but the correlation coefficients were lower than ISI in all cases (figure 4(b)) and the relationships were still site specific.

According to these results, the ISI index, despite being a simple difference index, can be considered the best index for monitoring grassland phytomass on a temporal basis,

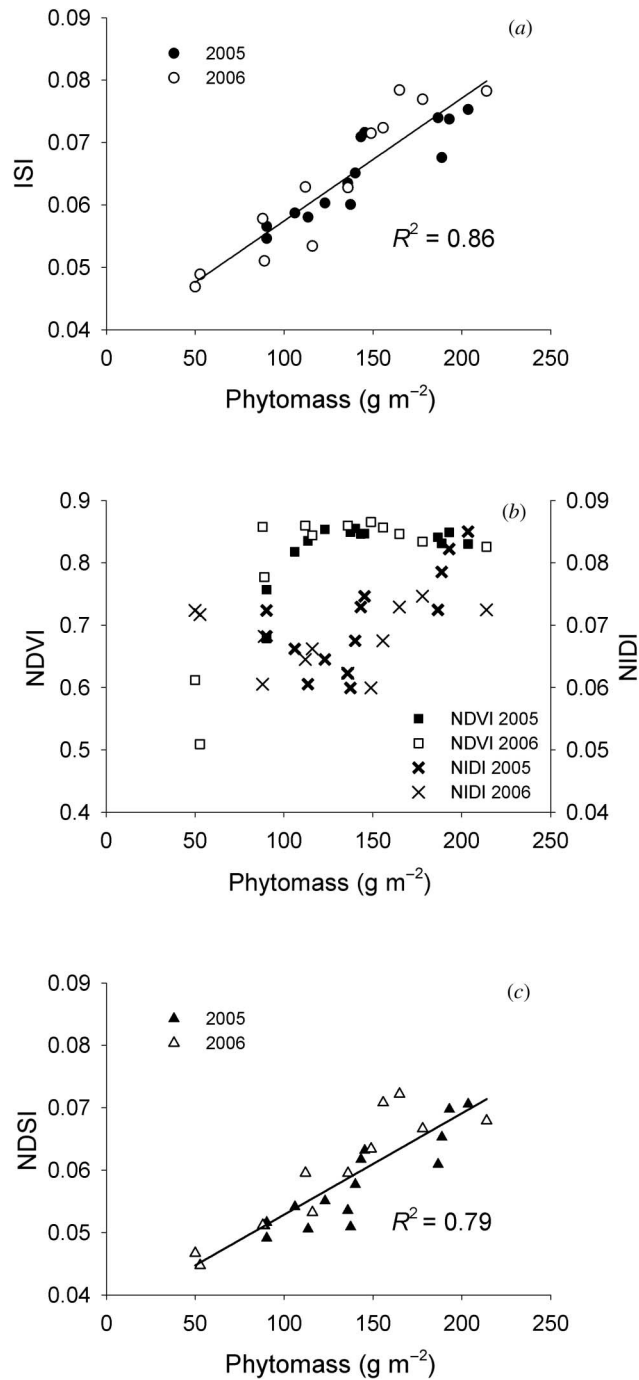


Figure 3. (a) ISI, (b) NDVI and NIDI and (c) NDSI relationships with phytomass at the Monte Bondone site ( $p < 0.01$ ).

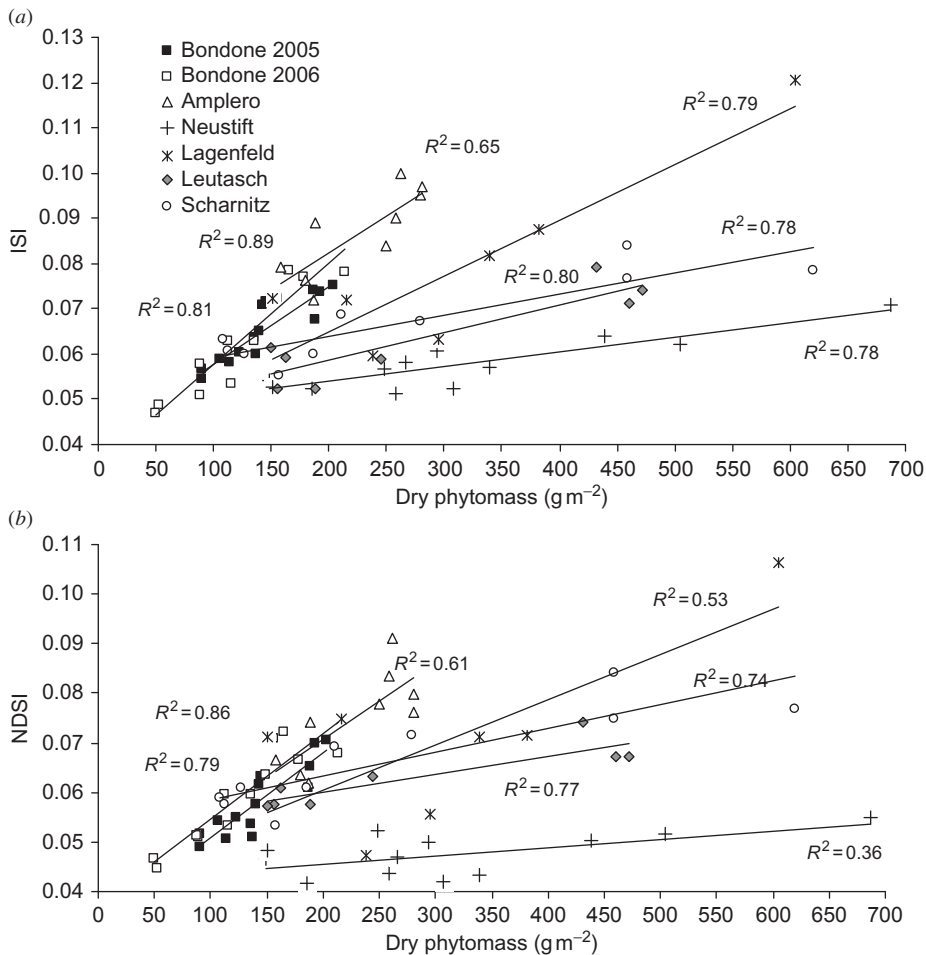


Figure 4. (a) ISI and (b) NDSI relationships at all investigated sites. All  $R^2$  are significant at  $p < 0.01$ .

essential for long-term monitoring sites where information about phenology, LAI and phytomass are needed.

The ISI performance was particularly surprising at the Amplero site, where the Mediterranean grassland curing effect (the typical vegetation browning-off during the dry season) was very strong. Despite this, the ISI increased during the entire growing season while other vegetation indices typically tended to decrease starting from June (data not shown), even if the phytomass was still increasing or stable.

### 3.4 WinSail modelling results

The WinSail model considers LAI as an input vegetation structure variable. According to the strong correlation ( $R^2 = 0.84$ ,  $p < 0.05$ ) found between LAI and phytomass in previous studies at Monte Bondone (Vescovo and Gianelle 2006), the results of the model can also be considered valid for phytomass. As a reference, at Monte Bondone,  $\text{phytomass} = 53.1(\text{LAI}) + 51.5$ .

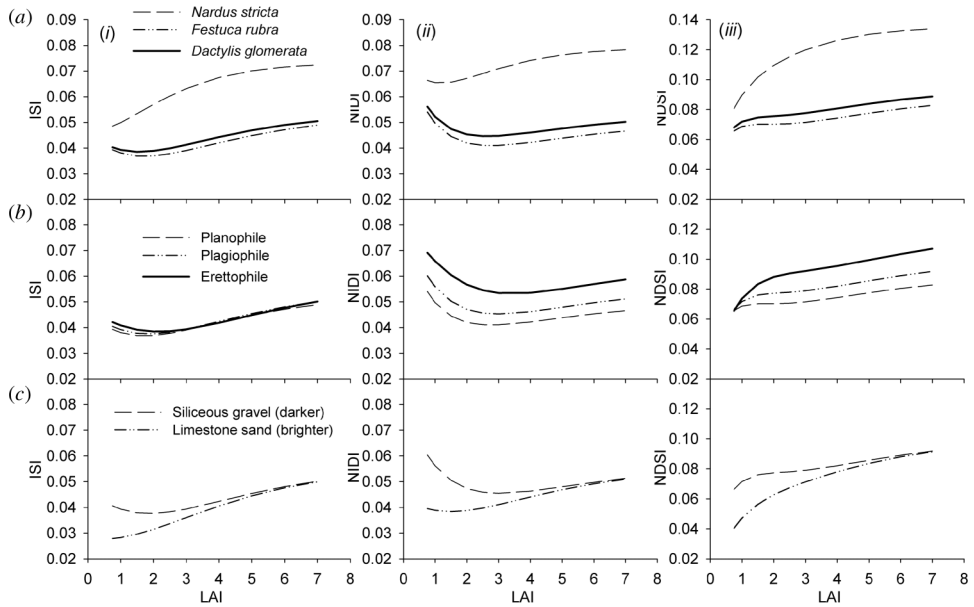


Figure 5. ISI (column (i)), NIDI (column (ii)) and NDSI (column (iii)) indices as a function of LAI simulated with the WinSail model: (a) for different species (with siliceous gravel background and uniform leaf area distribution, LAD); (b) for different leaf angle distributions (with *Festuca rubra* and siliceous gravel background); and (c) for different backgrounds (with *F. rubra* and uniform LAD).

Regarding the causes of ISI and NDSI site specificity, the WinSail model was able to point out some of the canopy characteristics, which can influence the dynamics of the reflectance in the ‘NIR shoulder’ range. Figure 5(a) shows the effect of species composition on the LAI dependency of ISI, NIDI and NDSI. While simulations with the optical properties corresponding to *F. pratensis* and *D. glomerata* were very similar, simulations for *N. stricta* resulted in significantly higher ISI and NDSI values. These marked distinctions are probably due to the typical *Nardus* leaf hardness and to its particular leaf internal structure, which strongly affects both the reflectance response and the indices trend. These results suggest that in grassland canopies, characterized by harder leaves and higher dry mass content (e.g. drier alpine grasslands, Mediterranean grasslands), both the angular coefficient and the intercept of the index–phytomass fit curve are expected to be higher, which corresponds to the data shown in figure 4.

In contrast to the findings of Jacquemoud *et al.* (2009) for the NIR reflectance values, the LAD (figure 5(b)) had little effect on the ISI–LAI relationship, while erectophile and plagiophile canopies seemed to appreciably increase NIDI and NDSI values. In the same way, different soil reflectances resulted in different index–LAI relationship slopes (figure 5(c)). According to the WinSail model results, ISI, NIDI and NDSI–LAI relationship slopes were higher for the limestone sand background (which was shown to be brighter than the siliceous gravel background). According to the model results, in grassland canopies characterized by different background reflectance, the brighter the background reflectance, the higher the angular coefficient of the index–phytomass relationship is to be expected.

#### 4. Summary and conclusions

The results of this article demonstrate that saturation of spectral vegetation indices is still a major problem for monitoring phytomass at full canopy cover, as was pointed out by many authors. On the contrary, our proposed indices (ISI and NDSI) showed good potential for monitoring even large amounts of above-ground phytomass.

For the investigated ‘traditional’ indices, saturation occurred earlier than had been previously reported (figure 1; Tucker 1977, Myneni *et al.* 1995, Gitelson *et al.* 1996, Ustin *et al.* 2004, Vescovo and Gianelle 2006). In fact, traditional indices such as the normalized difference vegetation index (NDVI), the EVI (both three band and two band), the WDRVI, the MSR and the RDVI showed clear signs of saturation for phytomass values higher than  $100 \text{ g m}^{-2}$ . It is worth noting that these indices (except NDVI) were specifically proposed to overcome the saturation problem. Furthermore, it is important to emphasize that both EVI and EVI 2, which are two new indices for vegetation monitoring at the global scale, did saturate at approximately the same levels as the other indices.

The infrared slope expressed as the ISI index was shown to be linearly related to grassland phytomass. With no signs of saturation occurring up to  $700 \text{ g m}^{-2}$  phytomass, ISI proved to be a valid option for monitoring the seasonal trend of canopy structural variables at full canopy cover. In fact, while visible–NIR indices (contrasting absorption and reflection mainly caused by the joint effect of pigments and leaf structure) saturated at full canopy cover, the proposed index focuses only on canopy structure (irrespective of photosynthetic capacity) and did not saturate. ISI was also shown to be suitable for monitoring phytomass in a strongly cured Mediterranean ecosystem, where the traditional indices perform poorly due to the high degree of browning of the herbaceous vegetation during summer drought.

Although ISI showed good potential for monitoring grassland structural variables on a temporal basis (without any signs of saturation), ISI and NDSI proved to be site-specific and as a consequence, not appropriate for monitoring spatial variability and mapping structural variables. NDSI (calculated as NDVI multiplied by NIDI), coupling a classic visible–NIR index with NIDI, was linearly correlated with phytomass, but the correlation coefficients were slightly lower than ISI. As shown by Hill (2004) for traditional visible–NIR vegetation indices, site specificity is one of the major factors limiting the estimation of grassland phytomass. The site specificity of visible–NIR indices is related to the presence of senescent material, to the background effect and soil colour. According to the WinSail modelling results of the present study, the site specificity of ISI and NDSI mainly resulted from grassland species composition and background reflectance. Higher values and slopes of the modelled index–phytomass relationships were shown to be related to the presence of hard-leaf grassland species (*N. stricta*) and to a brighter background. The WinSail simulations, in fact, explain why the Monte Bondone/Amplero angular coefficients and the intercepts of the index–phytomass relationships were considerably higher than for the other field sites: The Monte Bondone and Amplero field sites are characterized by a high presence of hard leaf species (typical of xerophile and low-nutrient grasslands), while the other sites (Neustift, Scharnitz, Leutasch and Längenfeld) are fertilized grasslands, composed of mesophile and hydrophile species. In order to experimentally test the hypothesis that species-specific differences in leaf internal structure are the main factors responsible for variation in the phytomass versus ISI/NDSI relationship and to disentangle this effect from others such as LAD and background reflectance, one

way forward would be to conduct hyperspectral reflectance measurements on mono-specific grasslands with differing leaf structures (hard vs. soft leaf species) sown on soils of differing brightness.

According to the analysed data, the ISI and the NDSI indices are suitable tools, at ground level, to monitor structural biophysical variables of grassland vegetation at full canopy cover on a temporal basis. These indices, following an appropriate on-site calibration, could be adopted in long-term temporal measurements, when information about grassland structural variables at the ecosystem level is needed on a continuous basis (e.g. in eddy covariance and phenology networks) and when the use of traditional indices does not appear feasible (in canopies which reach high LAI values). More research is needed in order to test the possibility of monitoring reflectance in the investigated NIR shoulder bands (to calculate ISI and NDSI indices) using specific multispectral sensors (such as SKYE SKR 1800 (Skye Instruments, Llandrindod Wells, Powys, UK) or CROPSCAN MSR16R (CROPSCAN, Inc., Rochester, MN, USA)) to be installed at the field sites for continuous measurements. Also, more studies are needed in order to test the possibility of extending these results to other vegetation types (forests, crops, etc.) and to perform these observations using imagery spectrometers (e.g. mounted on eddy covariance sites). Finally, further research is needed to verify the economic feasibility and the potential of using aircraft and satellite (e.g. Chris Proba) ISI/NDSI data as a proxy for grassland structural parameters.

### Acknowledgements

This research was supported by the EU project CARBOEUROPE-IP (GOCE-CT-2003-505572), the CARBOITALY project funded by the Italian government, the CfPAT project, Marie Curie 7<sup>o</sup> P.Q. – PCOFUND-GA-2008-226070 and the Austrian National Science fund (P17560-B03). The authors are very grateful for the assistance provided by the SpecNet community researchers.

### References

- BOEGH, E., SOEGAARD, H. and THOMSEN, A., 2002, Evaluating evapotranspiration rates and surface conditions using Landsat TM to estimate atmospheric resistance and surface conditions. *Remote Sensing of Environment*, **79**, pp. 329–343.
- CHEN, J., 1996, Evaluation of vegetation indices and modified simple ratio for boreal applications. *Canadian Journal of Remote Sensing*, **22**, pp. 229–242.
- COLWELL, J.E., 1974, Vegetation canopy reflectance. *Remote Sensing of Environment*, **3**, pp. 175–183.
- DELUCIA, E.H. and NELSON, K.P., 1993, Contribution of internal reflectance to light absorption and photosynthesis of shade leaves. *Bulletin of the Ecological Society of America*, **74**, pp. 211–212.
- EVERITT, J.H., ESCOBAR, D.E. and RICHARDSON, A.J., 1989, Estimating grassland phytomass production with near-infrared and mid infrared spectral variables. *Remote Sensing of Environment*, **30**, pp. 257–261.
- GAMON, J.A., RAHMAN, A.F., DUNGAN, J.L., SCHILDHAUER, M. and HUENNRICH, K.F., 2006, Spectral Network (SpecNet): what is it and why do we need it? *Remote Sensing of Environment*, **103**, pp. 227–235.
- GAO, X., HUETE, A.R., NI, W. and MIURA, T., 2000, Optical-biophysical relationships of vegetation spectra without background contamination. *Remote Sensing of Environment*, **74**, pp. 609–620.
- GIANELLE, D., VESCOVO, L., MARCOLLA, B., MANCA, G. and CESCATTI, A., 2009, Ecosystem carbon fluxes and canopy spectral reflectance of a mountain meadow. *International Journal of Remote Sensing*, **30**, pp. 435–449.

- GITELSON, A.A., 2004, Wide dynamic range vegetation index for remote quantification of crop biophysical characteristics. *Journal of Plant Physiology*, **161**, pp. 165–173.
- GITELSON, A.A., KAUFMAN, Y.J. and MERZLYAK, M.N., 1996, Use of a green channel in remote sensing of global vegetation from EOS-MODIS. *Remote Sensing of Environment*, **58**, pp. 289–298.
- GITELSON, A.A., VIÑA, A., MASEK, J.G., VERMA, S.B. and SUYKER, A.E., 2008, Synoptic monitoring of gross primary productivity of maize using Landsat data. *IEEE Geoscience and Remote Sensing Letters*, **5**, pp. 133–137.
- HILL, M., 2004, Grazing agriculture: managed pasture, grassland and rangeland. In *Remote Sensing for Natural Resources Management and Environment Monitoring*, S.L. Ustin (Ed.), pp. 449–530 (Hoboken, NJ: Wiley).
- JACQUEMOUD, S., VERHOEF, W., BARET, F., BACOUR, C., ZARCO-TEJADA, P.J., ASNER, C., FRANÇOIS, G.P. and USTIN, S., 2009, PROSPECT+SAIL models: a review of use for vegetation characterization. *Remote Sensing of the Environment*, **113**, pp. 56–66.
- JIANG, Z., HUETE, A.R., DIDAN, K. and MIURA, T., 2008, Development of a two-band enhanced vegetation index without a blue band. *Remote Sensing of Environment*, **112**, pp. 3833–3845.
- KNIPLING, E.B., 1970, Physical and physiological basis for the reflectance of visible and near-infrared radiation from vegetation. *Remote Sensing of Environment*, **1**, pp. 155–159.
- LEPRIEUR, C., VERSTRAETE, M.M. and PINTY, B., 1994, Evaluation of the performance of various vegetation indices to retrieve vegetation cover from AVHRR data. *Remote Sensing Reviews*, **10**, pp. 265–284.
- LIU, H.Q. and HUETE, A.R., 1995, A feedback based modification of the NDVI to minimize canopy background and atmospheric noise. *IEEE Transactions on Geoscience and Remote Sensing*, **33**, pp. 457–465.
- LIU, L., WANG, J., HUANG, W., ZHAO, C., ZHANG, B. and TONG, Q., 2004, Estimating winter wheat plant water content using red edge parameters. *International Journal of Remote Sensing*, **25**, pp. 3331–3342.
- MYNENI, R.B., FORREST, G.H., PIERS, J.S. and MARSHACK, A.L., 1995, The interpretation of spectral vegetation indices. *IEEE Transactions on Geoscience and Remote Sensing*, **33**, pp. 468–481.
- PILON, R., KLUMPP, K., CARRERE, P. and PICON-COCHARD, C., 2010, Determination of aboveground net primary productivity and plant traits in grasslands with near-infrared reflectance spectroscopy. *Ecosystems*, **13**, pp. 851–859.
- PINTY, B., LAVERGNE, T., WIDLÓWSKY, J.L., GOBRON, N. and VERSTRAETE, M.M., 2009, On the need to observe vegetation canopies in the near-infrared to estimate visible light absorption. *Remote Sensing of Environment*, **113**, pp. 10–23.
- PRICE, J.C., 1993, Estimating leaf area index from satellite data. *IEEE Transactions on Geoscience and Remote Sensing*, **31**, pp. 727–734.
- PRINCE, S.D., 1991, A model of regional primary production for use with coarse-resolution satellite data. *International Journal of Remote Sensing*, **12**, pp. 1313–1330.
- ROSENQVIST, A., MILNE, A., LUCAS, R., IMHOFF, M. and DOBSON, C., 2003, A review of remote sensing technology in support of the Kyoto Protocol. *Environmental Science and Policy*, **6**, pp. 441–55.
- ROUJEAN, J.L. and BREON, F.M., 1995, Estimating PAR absorbed by vegetation from bidirectional reflectance measurements. *Remote Sensing of Environment*, **51**, pp. 375–384.
- ROUSE, J.W., HASS, R.H., SHELL, J.A. and DEERING, D.W., 1974, Monitoring vegetation systems in the great plains with ERTS-1. In *Proceedings 3rd Earth Resources Technology Satellite Symposium*, 10–14 December 1974, Washington, DC (Washington: NASA), Vol. 1, pp. 309–317.
- SELLERS, P.J., 1985, Canopy reflectance, photosynthesis and transpiration. *International Journal of Remote Sensing*, **6**, pp. 1335–1372.

- SLATON, M.R., HUNT JR., E.R. and SMITH, W.K., 2001, Estimating near-infrared leaf reflectance from leaf structural characteristics. *American Journal of Botany*, **88**, pp. 278–284.
- THENKABAIL, P.S., SMITH, R.B. and DE PAUW, E., 2000, Hyperspectral vegetation indices and their relationships with agricultural crop characteristics. *Remote Sensing of Environment*, **71**, pp. 158–182.
- TUCKER, C.J., 1977, Asymptotic nature of grass canopy spectral reflectance. *Applied Optics*, **16**, pp. 1151–1156.
- TUCKER, C.J., 1979, Red and photographic infrared linear combination for monitoring vegetation. *Remote Sensing of Environment*, **8**, pp. 127–150.
- USTIN, S.L., JACQUEMOUD, S., ZARCO-TEJADA, P.J. and ASNER, G.P., 2004, Remote sensing of the environment: state of the science and new directions. In *Remote Sensing for Natural Resources Management and Environment Monitoring*, S.L. Ustin (Ed.), pp. 679–729 (Hoboken, NJ: Wiley).
- VAN LEEUWEN, W.J.D. and BARRON, J., 2006, Spectral vegetation indices and uncertainty: insights from a user's perspective. *IEEE Transactions on Geoscience and Remote Sensing*, **44**, pp. 1931–1933.
- VESCOVO, L. and GIANELLE, D., 2006, Mapping the green herbage ratio of grasslands using both aerial and satellite spectral reflectance. *Agriculture, Ecosystems and Environment*, **115**, pp. 141–149.